Design and measurement of a reference source at lower frequencies

Cédric Pinhède, Philippe Herzog

DESIGN AND MEASUREMENT OF A REFERENCE SOURCE AT LOWER FREQUENCIES

Cédric Pinhède[1] **and Philippe Herzog**[2]
[1] LMA - CNRS, 4 impasse Nikola Tesla, 13013 Marseille, France
[2] ARTEAC-LAB SAS, 8 allée Léon Gambetta, Place de l′innovation (CIC), 13001 Marseille, France
pinhede@lma.cnrs-mrs.fr

ABSTRACT

A reference source may be needed for comparison with an unknown one in non-anechoic environment or for estimating the incident pressure in free field. However, the performance of such a source must be assessed in an anechoic room, which is not perfect below its cut-off frequency (usually 70 to 100 Hz). This presentation deals with the design of a reference source targeting lower audio frequencies (40-200 Hz), involving two loudspeakers combined in "push-pull". This source features an internal microphone allowing to estimate its volume velocity, which can be related to the radiated pressure. The second part of the presentation deals with the acoustic characterization of this source, which raise many difficulties as no facility can be considered as truly anechoic in the lower part of the targeted frequency band. These difficulties will be presented and discussed, showing the trade-off which had to be found and the resulting measurements.

1. INTRODUCTION

Calibrated sources are used for a wide variety of applications, *e.g.* for wall transparency measurements, room acoustics, power and radiation measurements. The latter case is illustrated by a standard for loudspeaker measurements [1], which suggest that when the available facility is not fully anechoic over the effective frequency range, *"... the loudspeaker under test is removed from the chamber and replaced by a calibrated reference loudpseaker ..."*. Such a "reference loudpseaker" has to be calibrated using a larger facility, or by other means.

Another need for a reference source, although far from widespread yet, has motivated our study : it is a mandatory ressource for the identification of the operator linked to the diffraction by surrounding walls, potentially used for active anechoicity techniques [2]. Again, what is needed here is a source which radiated pressure may be known in 3D space with a sufficient accuracy.

These needs differ from reference sources designed for power measurements, which must be powerful but cannot usually be driven by an arbitrary signal. They also differ from sources designad for building acoustics, which achieve an uniform power radiation pattern but do not allow to predict the pressure in an arbitrary location with a sufficient accuracy.

A simple concept of the targeted reference source is an omnidirectional source, as it is convenient to use and to calibrate. It should also be compact (all dimensions small compared to the shortest wavelength of interest) in order to have minimal diffraction by its body, thus reducing second order diffraction in a non anechoic environment. Last, it should be able to reproduce a wide range of signals, especially at lower frequencies as this is the frequency range targeted by the two last applications mentionned above. This incites to consider a loudspeaker system combining a few low frequency (LF) drivers inside a small enclosure, designed so that it can reach low frequencies with a good linearity.

2. DESIGN

The simplest design considered was a simple closed box loading a LF driver, as depicted in Fig. 1(a). It would be adequate at very low frequencies, although its acoustic center is not well defined and may slightly move with frequency.

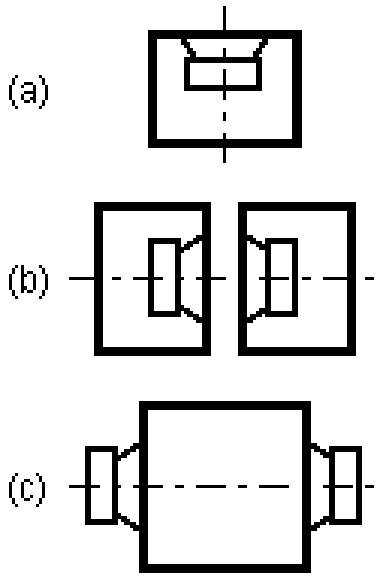

Figure 1. Various design geometries

A simple way to compensate for this problem is to place two such closed enclosures face to face, as in Fig. 1(b) : the

radiation then occurs through the annular spacing between the two sources. This principle is used by several laboratory and commercial units. Its main drawbacks are : (1) the total length of the source may lead to some diffraction and (2) it is difficult to estimate accurately its volume velocity, which may be slightly different between the two speakers.

The final design was therefore based on a single volume shared by two speakers, as in Fig. 1(c). The internal pressure is then proportional to the overall volume velocity and the acoustic coupling between the speakers should also reduce the influence of their slight differences. The drawback of this design is however that radiation occurs through two annular surfaces instead of a single one. Moreover, the source was designed with a parallelepipedic enclosure instead of the ideal cylindrical (or spherical) one, as it was much easyier to build. This may of course degrade somewhat the radiation pattern.

The reference source presented thereafter is designed in order to approximate a compact monopole in the frequency range $[40 - 200]$ Hz. It features a very stiff enclosure, almost cubic, supporting two powerful woofers mounted face to face with their motors outside the volume. The radiating surfaces are then constituted by the clearances in each driver basket, as can be seen in Fig. 2.

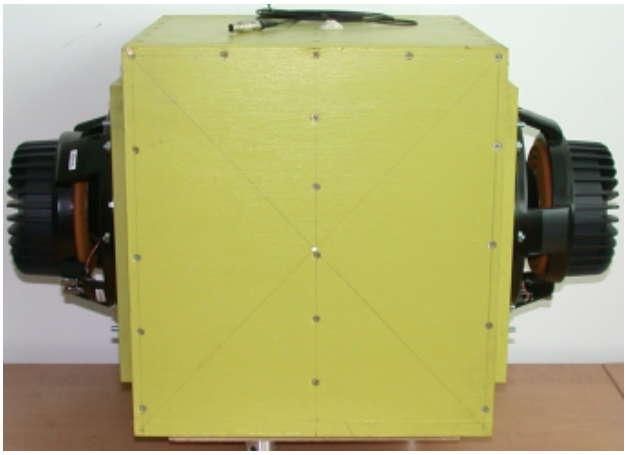

Figure 2. The reference source

2.1 Loading volume

The source features two loudspeakers fixed face to face and wired in series. The internal dimensions are: 350 mm height, 350 mm width, 320 mm depth. The total internal volume V_s is therefore 42.4 l, a relatively small volume compared to the one recommended as optimum, using the Thiele/Small model [3]. Although this has a negative effect on the cut-off frequency, eventually requiring an equalization, it enforces a strong acoustic coupling between the two speakers, thus reducing the effect of their compliance differences.

The small closed loading volume also leads to a high internal acoustic pressure, which acts on the walls. In order to limit their vibration or leakages, which could have an adverse contribution to the source radiation, several precautions were taken :

- The walls are made of 18 mm thick plywood panels, which are glued, screwed and painted.
- The two speakers are linked to each other using metallic rods, so that the forces generated by the two drivers cancel out.
- A central stiffener is added, made of a square panel with a circular aperture at its center. It also supports the internal microphone.

Figure 3. The internal reference source

These building rules are illustrated by Fig. 3; they allow to bear the efforts resulting from the large membranes displacement at lower frequencies, while avoiding any significant parasitic radiation of the walls.

2.2 Loudspeakers

The two speakers are 10” units manufactured by Beyma (model 10LW30/10). Eight samples of this model were ordered and tested. After a long enough burn-in, some Thiele-Small (T/S) parameters were measured individually. The two units kept for the source (references HauP0078 and HauP0079) have been selected in order to have a mechanical quality factor and a resonance frequency as close as possible, see Tab. 1.

	F_s	R_{es}	Q_{ms}	R_e
HauP0078	56.8	123.7	8.11	7.43
HauP0079	56.0	164.9	8.9	7.59

Table 1. Parameters Thiele-Small

To further assess the actual symmetry of the source, the mechanical behaviour of the two loudspeakers (mounted

on the enclosure) was measured using a laser displacement sensor (Keyence, model LK-G32). Fig. 4 presents the transfer functions between the voltage across the loudspeakers (connected in series) and the displacements of their membranes.

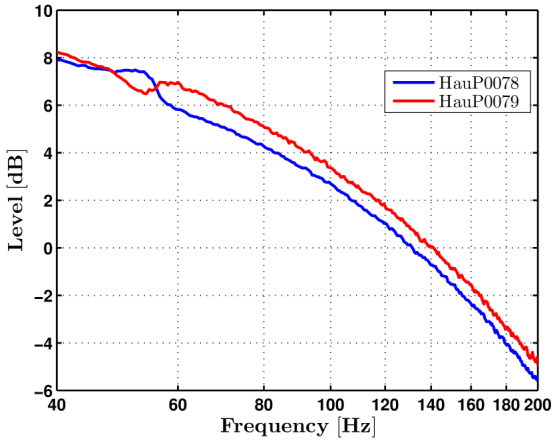

Figure 4. The transfer function between displacement and voltage of loudspeaker mounted in the reference source.

The global trend is a damped low-pass behaviour, as could be expected from the T/S model. There is an irregularity around 55 Hz : this seems to result from the difference between the suspensions compliances, combined with an internal mode of the enclosure. The two displacements are however very close to each other : their difference does not exceed 1 dB.

3. RADIATED PRESSURE ESTIMATE

A high pressure microphone (GRAS model 40BF) was fitted at the geometric center of the enclosure, suspended by an elastic band, see Fig. 3. This microphone provides a measurement p_{int} of the internal acoustic pressure. This measurement is used as a reference to estimate the source volume velocity and indirectly estimate the pressure radiated by the source in free field.

Assuming almost isobaric compression inside the closed box, the overall volume velocity Q_s output by the two loudspeakers may be estimated from the internal acoustic pressure p_{int} in the volume :

$$Q_s = -\imath\omega C_{ab} p_{int} \tag{1}$$

where ω is the angular frequency, a time dependence $\mathrm{e}^{\imath\omega t}$ is assumed, and C_{ab} is the compliance of the volume :

$$C_{ab} = \frac{V_s}{\rho_0 c^2} \tag{2}$$

where ρ_0 is the air volumic mass. Hence :

$$Q_s = \frac{-\imath\omega V_s}{\rho_0 c^2}\, p_{int} \tag{3}$$

The assumption behind this relation is that the volume is compact enough so that a single (isobaric) mode describes the internal field with enough accuracy. This is only valid at lower frequencies, approximately up to 200 Hz.

3.1 Monopole approximation

At frequencies low enough so that the distance between the drivers may be neglected, and neglecting also the diffraction by the source body, the radiated pressure may be approximated by a monopole with the overall volume velocity Q_s. The radiated pressure at a measurement point M, for source $\tilde{S}$ at location S_0, is thus :

$$p_{inc}(\tilde{S}, M) = \frac{\imath\omega\rho_0 Q_s}{4\pi}\, \frac{\mathrm{e}^{-\imath kr(S_0,M)}}{r(S_0,M)} \tag{4}$$

The pressure at any point M may then be estimated using the internal pressure p_{int} :

$$p_{inc}(\tilde{S}, M) = p_{int}\, \frac{\omega^2 V_s}{4\pi c^2}\, \frac{\mathrm{e}^{-\imath kr(S_0,M)}}{r(S_0,M)} \tag{5}$$

Beside the usual geomatrical spreading of a spherical wave, this relation emphasizes that the internal pressure is proportional to the membranes displacement while the radiated pressure is proportional to their accelerations - hence the ω^2 factor.

3.2 Dual pole model

At higher frequencies, the two loudspeakers can no more be considered as a single punctual source. However each one is small enough compared to the wavelengths of interest so that it may be assimilated to such a pole. The source $\tilde{S}$ is therefore represented by two monopoles S_1 and S_2, assumed to have identical volume velocities and phases. Although this is not strictly exact, as depicted in Fig. 4, it allows to use a single reference signal for both loudspeakers : each pole is assumed to have half the volume velocity estimated through the internal pressure p_{int}.

The positions of these two monopoles are deduced from geometrical measurements. For the source presented here, their positions are estimated each 0.3 m away from the center S_0 of the source. The radiated pressure at a measurement point M can thus be approximated by the following relation :

$$p_{mod}(\tilde{S}, M) = p_{int}\, \frac{\omega^2 V_s}{8\pi c^2}\, \{\frac{\mathrm{e}^{-\imath kr(S_1,M)}}{r(S_1,M)} + \frac{\mathrm{e}^{-\imath kr(S_2,M)}}{r(S_2,M)}\} \tag{6}$$

The far field directivity pattern of the source is then no more omnidirectional. The difference with a single monopole is even greater at usual measuring ranges, which cannot be considered as large compared to the source dimensions.

As an example, Fig. 5 presents the radiation pattern for a receiver M at 1 meter distance from the source $\tilde{S}$, for 5 frequencies. The angular reference (0 °) is the axis common to both loudspeakers. Depending on the angle and frequency, the pressure differs from a monopole by $[0.5 - 3]$ dB. Below 120 Hz, the radiation pattern is very

close to the one of a single monopole source (dotted curve), although there is a difference because of the short measuring distance. At higher frequencies, the two-pole model is mandatory to reach a good accuracy.

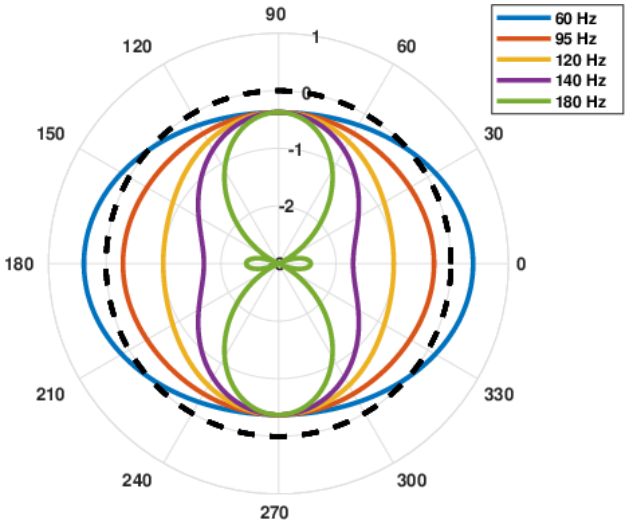

Figure 5. The radiation pattern of two monopoles for 5 frequencies

4. CHARACTERIZATION OF THE SOURCE

The acoustic characterization of the above described prototype reference source was carried out in an anechoic room at the Laboratoire de Mécanique et d'Acoustique (LMA). Measurements of the directivity of the source were performed in an horizontal plane passing at the geometry center of the source, see Fig. 6. The setup was controlled using a laser theodolite (Leica, model TCR407 : an optic instrument for triangulation position measurements) allowing accurate recording of the relative positions of each object for the purpose of post-processing.

A turntable (Newport, model RV240CC) controlled by a controller (Newport, model ESP300) was installed just above the floor wedges. It moved a stiff truss stand, allowing to shift the measurement plane at a height of about $z_0 = 1.57$ meter. The source was centered on this setup, so that it could rotate around its geometric center. A microphone (GRAS, model 40AF) was positioned at the point M_0 located at a height 1.56 meters and at a distance $r = 1.04$ meters from the source.

4.1 Validation of the source model

Transfer function measurements were performed at angular steps of 5 degrees. Fig. 7 presents, as a function of frequency, the amplitude of the relative difference $Err = \frac{p_{meas}}{p_{mod}}$, averaged over a full circle, between the pressure measured at the point M_0 and the one estimated from the internal pressure.

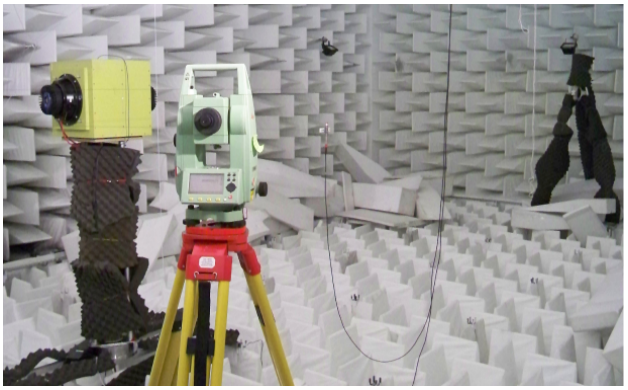

Figure 6. The anechoic room at LMA

The dotted grey curve represents this difference when using the single monopole model (Eqn. (5)). The model diverges from the measurements, especially at higher frequencies : Err shows a steep decreasing slope down to about -3.5 dB at 200 Hz. There are also irregularities : The cut-off frequency of the anechoic room is about 70 Hz, leading to a modal behaviour at lower frequencies. Moreover, previous studies showed that the facility lining is not perfect, generating significant artifacts between 130 and 150 Hz [4, 5].

The blue line corresponds to the dual pole model (equation 6). This improved model leads to lower difference for the considered measurement position : Err stays within $[-0.5; 0.5]$ dB over the frequency bands $[70 - 130]$ and $[150 - 180]$ Hz - but it is still in excess of 1 dB at higher frequencies, and reaches about 1.5 dB around 140 Hz.

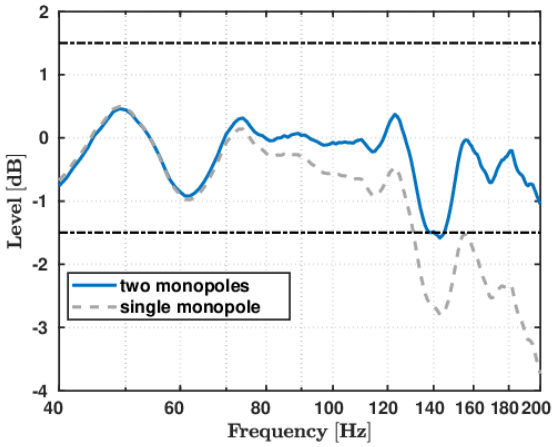

Figure 7. The error Err (levels in dB) as a function of frequency, averaged over all angles

The two models give similar Err values lower frequencies, up to about 70 Hz : this is consistent with our hypothesis. In both cases, the Err fluctuations are probably related to the non-anechoic behaviour of the facility (below its cut-off), as the isobaric model has been checked against more sophisticated estimation methods [6].

The large artifact around 140 Hz is also present for

both models; it is likely to be related to the anechoic room performance, as stated above, although this cannot be assessed rigorously.

4.2 Angular discrepancies

Angular fluctuations are given in Fig. 8 and 9 which presents at 4 frequencies the relative error Err as a function of the incident angle, for the single and dual pole models respectively.

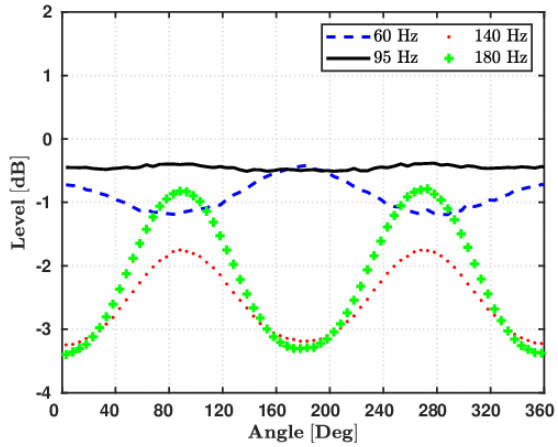

Figure 8. Error Err (in dB) as a function of angle for the single pole model, at 4 frequencies

The single pole model (Fig.8) leads to a significant angular error, in addition to the decrease of level with frequency. The measured level is lower than predicted when the microphone is facing each loudspeaker (0 and 180 °) : For such an orientation, one loudspeaker is much closer than the other, and is the single one to contribute significantly to the measured pressure. When the loudspeakers are at a comparable distance, their contributions add up, leading to an increased presure. Moreover the distance to the nearest radiating area changes very significantly with the angular position, while it is assumed constant in the single pole model. This error increases with frequency, as diffraction and directivity start to be significant.

For the dual pole model (Fig. 9), the average values of the Err difference are close to 0 dB at 95 Hz. They are larger than 0.5 dB around 60 and 140 Hz, as observed in Fig.7, but their angular variations are comparatively much smaller, even if it increases around 180 Hz. The overall performance of the dual pole model is better than the single pole one, as expected.

4.3 Calibration of the source

As the dual pole model leads to relatively small angular differences with the measured pressure, a logical step is to compensate the averaged frequency response of Fig. 7; *e.g.* by using a frequency equalization file. This calibration step removes the greatest part of the error shown in Fig. 9, resulting in the performances depicted by Fig. 10.

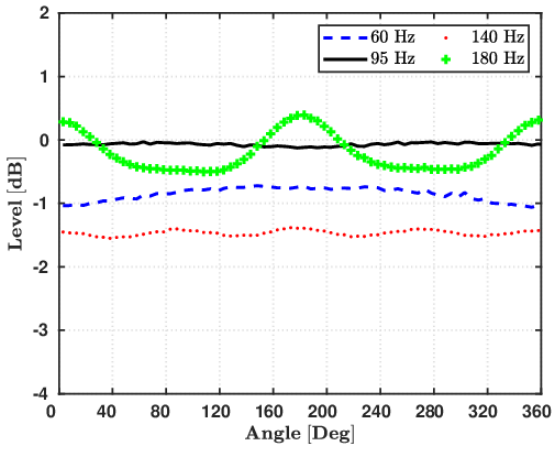

Figure 9. Error Err (in dB) as a function of angle for the dual pole model, at 4 frequencies

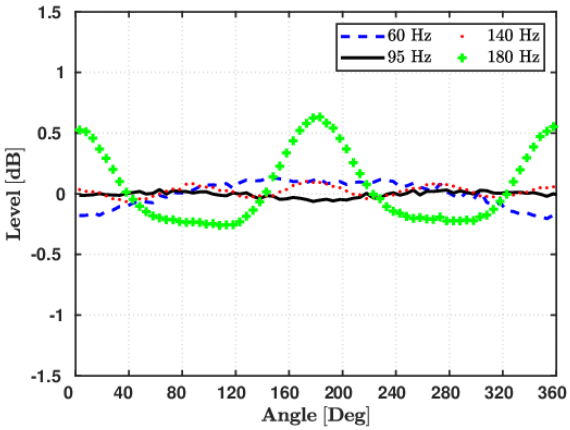

Figure 10. Error Err (in dB) as a function of angle for the dual pole model, at 4 frequencies, after frequency calibration.

This figure shows that the calibrated dual pole model is quite satisfying, leading to a residual difference between model and measurements smaller than 0.2 dB at 60, 95 and 140 Hz. It is however much larger at 180 Hz, reaching about 0.55 dB : the oscillating pattern at this frequency seems to be related to a bad estimation of the poles distance, which may be different at higher frequencies because of the diffraction of the driver motors, and there may also be a result of the slight dissymetry of the source.

To assess the suitability of the model, Fig. 11 shows, for all frequencies, the maximal value among all angles of the difference between the calibrated dual pole model and the pressure measured at M_0. It is lower than 0.3 dB from 50 Hz to 140 Hz, then increasing regularly to reach about 0.8 dB at 200 Hz. This shows that the calibrated dual pole model is sufficient to characterize the proposed reference source with a good accuracy at low frequencies (at least between 50 Hz and 140 Hz). The results shown in Fig. 10 suggest that this model could be improved above 140 Hz, *e.g.* by identifying a pole distance slightly depending on

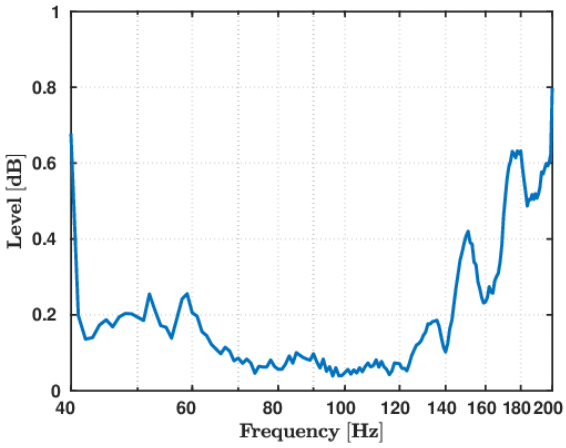

Figure 11. Maximal error Err (in dB) among all angles, as a function of frequency, using the calibrated dual pole model

frequency. This has however to be further investigated.

5. VALIDATION IN ANECHOIC ROOM

Following the calibration step, the source $\tilde{S}$ has been tested, at the same position in the same anechoic room, but using different microphone positions. For this measurement, the source axis (defined by the two poles corresponding to the loudspeakers) was put horizontally along the room longest dimension. A motorized cable was then used for moving the microphone along a line parallel to the source axis. This defined several microphone positions, at various distances and angles from the source. Fig. 12 represents, in the horizontal plane of the anechoic room, the successive positions of the microphone by blues points and the position of the reference source $\tilde{S}$ by a black circle. The red cross represents the position of microphone M_0 which was used for the calibration, while rotating the source.

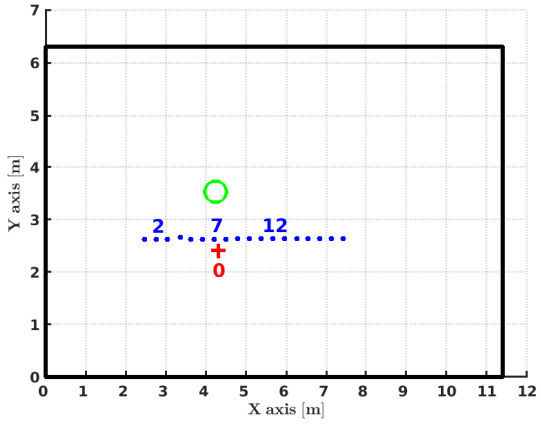

Figure 12. The geometry of device in anechoic room

Coordinates of the source and microphone positions were again recorded using the theodolite (Leica, model TCR407). Table 2 presents, for three points, the distance and the angle between the the source and the microphone positions. Point M_2 is close to the room door, point M_7 is close to the location M_0 used for characterization of $\tilde{S}$ and point M_{12} is approximately symmetric of M_2 with respect to M_7.

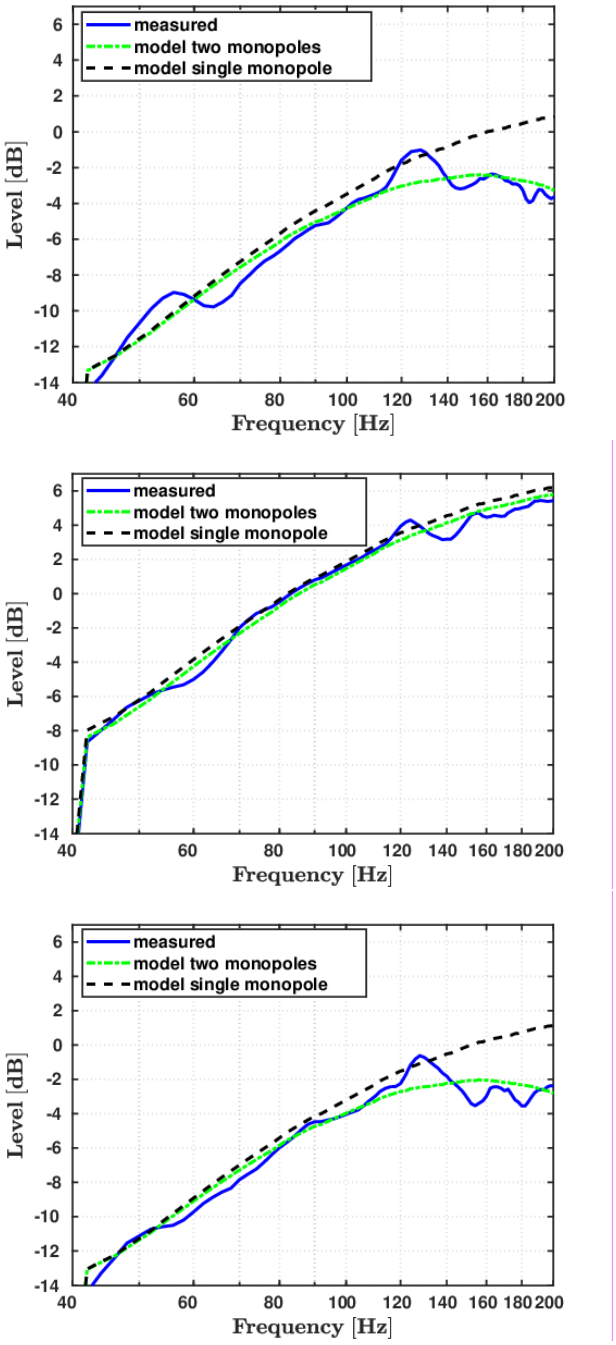

Figure 13. Pressure at three microphones positions, in an anechoic room : M_2 (upper), M_7 (middle), M_{12} (bottom)

Fig. 13 presents, at microphone positions M_2, M_7 and M_{12} the comparison of the measured pressure levels - represented by the blue curve - and the pressure levels estimated using the single (dotted black) and dual (green)

pole models. As for the calibration, some irregularities can be noticed below 80 Hz and around 130 Hz. Clearly the dual pole model is closer to the measured pressure, especially at frequencies above 80 Hz.

Position	M_2	M_7	M_{12}
Distance r	1.76 m	0.95 m	1.71 m
Angle θ	147°	92°	34°
Height z	1.32 m	1.26 m	1.24 m

Table 2. Distances and angles between the source $\tilde{S}$ and the positions (M_2, M_7, M_{12})

Fig. 14 presents the relative error at the three points M_2, M_7 and M_{12}, *i.e.* the ratio (in dB) of the measured pressure to the pressure estimated using the dual pole model. In this figure, no frequency calibration is taken into account : the irregularities at both ends of the frequency band are therefore similar to the ones already observed, although they are not identical for all three locations.

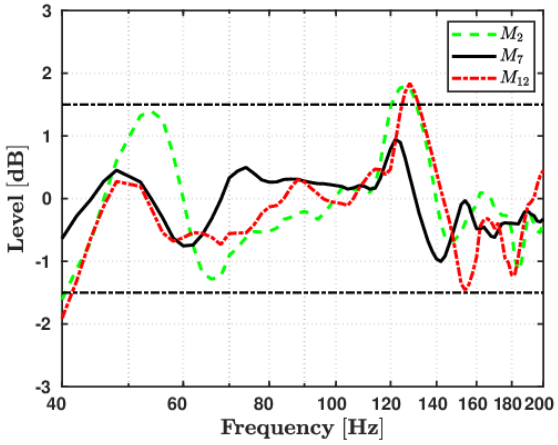

Figure 14. Err at positions M_2, M_7, M_{12} , without calibration

Taking into account the frequency calibration (*i.e.* the average over all angles depicted by Fig. 7) is supposed to improve the relative error. Fig. 15 thus presents the same relative error as Fig. 14, but using the calibration.

As expected, the relative error is significantly improved at M_7 : although the calibration is computed for an average at all angles, it has a beneficial contribution in the single direction presented here, reducing the relative error below about 0.5 dB at all frequencies. However, the calibration does not compensate fully the relative error at M_7.

This difference is emphasized by Fig. 16, which presents the same calibrated relative error, but comparing M_0 and M_7 which are very close to each other (thus at almost the same angle and distance). Note that these two measurements have also been performed at very different times (several weeks between them), so that they also allow to estimate the reproducibility of the calibration. Rel-

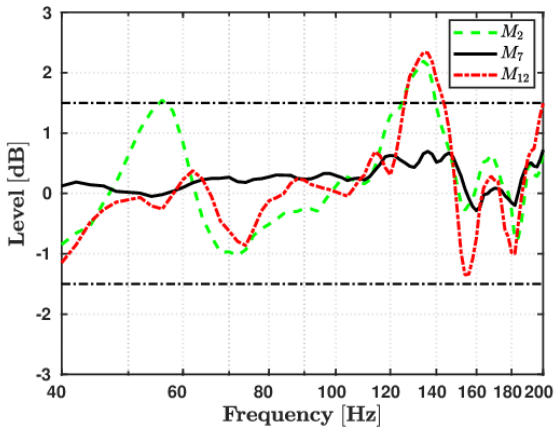

Figure 15. Err at positions M_2, M_7, M_{12}, after calibration

ative error is indeed lower for M_0 (which was part of the dataset used for the calibration) than for M_7, especially at frequencies above 110 Hz. Some non stationary processes might not be taken into account by the calibration procedure (*e.g.* temperature dependancy of C_{ab}).

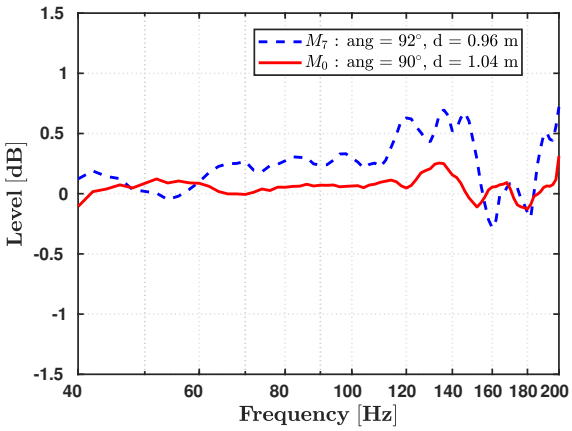

Figure 16. Err at positions M_0 and M_7, after calibration

The effect of the calibration is still less convincing for locations M_2 and M_{12} : no significant improvement of the relative error is observed - it may even be considered as worse after calibration. This contrasts with the improvement at M_7. An explanation is given considering Fig. 12 : while M_7 is very close to M_0, M_2 and M_{12} are both at a larger distance and different angles from the source.

However, as these locations have been chosen symetrically with respect to the source, they should behave in a similar way. Quite the opposite, they exhibit different variations of their relative errors, at lower frequencies and even more around 140 Hz : this corresponds with the known limitations of the anechoic room [4, 5]. This last remark leads to suspecting that the calibration has been contaminated by the non perfect behaviour of the anechoic room, even if other additional causes cannot be ruled out.

6. CONCLUSION

This paper presents the design of a reference source allowing to determine the pressure it radiates in free field at low frequencies. The design results from a trade-off between a sufficient volume velocity, requiring large loudspeakers and loading volume, and a compact body allowing to reduce the diffraction effects and leading to a simple radiation model.

This radiation model has been improved by taking into account the two radiation areas resulting from the chosen structure. It allows to link the radiated pressure to the pressure inside the single loading volume, measured by a suitable microphone. This model is required above 80 to 100 Hz, giving then a better estimate than a model assuming a single monopole.

A calibration might still improve the model; we tested a calibration procedure based on the frequency dependance of the response averaged over a circle of measurement points. This however requires to be able to perform anechoic measurements at quite low frequencies. The anechoic room we used does not seem sufficient for that purpose. A new calibration campaign should be planned in the new LMA facility, which has a much better performance than the one available for this work. Alternatively, methods less sensitive to the actual room performances could be used [6, 7].

Further improvement of the calibration will also necessitate to better understand the differences between measurements made at several weeks time intervals : non stationary phenomena may need to be controlled or compensated.

7. REFERENCES

[1] IEC, *IEC268-5 Standard : Sound system equipment, Part 5 : loudspeakers - Amendment 2*, 1996.

[2] D. Habault, E. Friot, P. Herzog, and C. Pinhède, "Active control in an anechoic room : Theory and first simulations," *Acta Acustica united with Acustica*, vol. 103, no. 3, pp. 369–378, 2017.

[3] R. Small, "Closed-box loudspeaker systems part i: Analysis," *J. Audio Eng. Soc.*, vol. 20, no. 10, pp. 798–808, 1972.

[4] M. Melon, C. Langrenne, D. Rousseau, and P. Herzog, "Comparison of four subwoofer measurement techniques," *J. Audio Eng. Soc.*, vol. 55, no. 12, pp. 1077–1091, 2007.

[5] S. Schneider and C. Kern, "Acoustical behavior of the large anechoic chamber at the laboratoire de mécanique et d'acoustique in the low frequency range," *Acta Acustica united with Acustica*, vol. 94, pp. 141–147, 01 2008.

[6] M. Melon, C. Langrenne, and P. Herzog, "Evaluation of a method for the measurement of subwoofers in usual rooms," *J. Acoust. Soc. Am.*, vol. 127, no. 1, pp. 256–263, 2010.

[7] M. Sanalatii, P. Herzog, R. Guillermin, M. Melon, N. Poulain, and J.-C. Le Roux, "Estimation of loudspeaker frequency response and directivity using the radiation-mode method," *J. Audio Eng. Soc.*, vol. 67, no. 3, pp. 101–115, 2019.